Guidance Navigation and Control Techniques for 4D Trajectory Optimization Satisfying Waypoint and No-Fly Zone Constraints

(Article begins on next page)

18 April 2024

Guidance Navigation and Control Techniques for 4D Trajectory Optimization Satisfying Waypoint and No-Fly Zone Constraints

Daniele Giuseppe Mazzotta[1]
Politecnico di Torino, Turin, Italy, 10129

The main purpose of this research is to develop a new FMS (Flight Management System) to control a commercial airliner along an optimized 4-Dimensional Trajectory (4DT), respecting time and path constraints, and avoiding a No-Fly Zone (NFZ). The optimum, expressed in terms of minimum fuel consumption, is addressed by solving an Optimization Control Problem (OCP) by means of a numerical direct collocation scheme, namely the *Chebyshev Pseudospectral* method. The OCP trajectory solution is a discrete sequence of optimal aircraft states which guarantee the *minimum-fuel* trip between two waypoints. With the aim of controlling the aircraft along lateral, vertical and longitudinal axis , and in order to respect NFZ and waypoints constraints along the optimum 4DT, different guidance navigation and control techniques were implemented. In order to validate the effectiveness of this algorithms on the Boeing 747-100 Automatic Flight Control System (AFCS), when it has to follow a 4D cruise route, several simulations were performed by generating three FMSs in the Multipurpose Aircraft Simulation Laboratory (MASLab), a software implementing the flight dynamic model of the Boeing 747-100.

Nomenclature

4DT	=	4-dimensional trajectory	OCP	=	optimal control problem
A/C	=	aircraft	ODE	=	ordinary differential equation
A/T	=	autothrottle	R	=	along path distance
ADM	=	aircraft dynamic model	$RNAV$	=	area navigation
AFCS	=	automatic flight control system	t	=	time
AGL	=	above ground level	TLA	=	throttle lever angle
APD	=	along path distance	$TNAV$	=	time navigation
ATC	=	air traffic control	TOA	=	time of arrival
C	=	path constraints	T_j	=	Chebyshev polynomial of jth order
CGL	=	Chebyshev-Gauss-Lobatto	$u(t)$	=	vector of control variables
CTA	=	controlled time of arrival	V_{TAS}	=	true air speed
ETA	=	established time of arrival	WP	=	waypoint
FMS	=	flight management system	w	=	Clenshaw-Curtis weights
IM	=	interval management	$x(t)$	=	vector of state variables
IAS	=	indicated air speed	Ψ	=	Mayer term of cost function
J	=	cost function	ψ	=	boundary conditions; heading angle
l_j	=	Lagrange polynomial of jth order			
L	=	Lagrange term of cost function	*Subscripts*		
LGM	=	lateral guidance manager	0	=	initial time
LNAV	=	lateral navigation	d	=	desired target
M	=	Mach number	f	=	final time
NFZ	=	no-fly zone	l	=	lower bound
NLP	=	nonlinear programming problem	u	=	upper bound

---
[1] Ph. D. Student, Department of Mechanical and Aerospace Engineering, daniele.mazzotta@polito.it

I.   Introduction

The guidance and control of an aircraft for the 4DT navigation, has commonly faced the problem of researching and studying the laws describing the dynamic behavior of the vehicle, as realistic and detailed as possible. An additional difficulty is represented by the time constraints which define the 4D route. After a negotiation process between the aircraft (A/C) and the Air Traffic Control (ATC) network, the A/C has to be controlled to respect the Time of Arrival (TOA) at a metering point of a canonical 3D route. The trajectory prediction for the 4DT navigation has a strong impact on the environment, as well as on the operations of the partners involved in the air transport sector. To generate and perform greener trajectories in terms of fuel consumption, emissions and perceived external noise, a trajectory optimization is required. In this context, Politecnico di Torino is developing an optimization tool that will be integrated in the next generation Flight Management System (FMS). With this extended capability, the FMS will be able to address both the trajectory optimization and the control of the A/C toward the optimum target.

In research, there are many examples of innovative mathematical methods providing, quasi-real time, the optimum targets to achieve a minimum fuel trajectory. In this work, the trajectory optimization is achieved by employing the Chebyshev pseudospectral method. This method is based on discretizing both time history and state variables of a given control system, transforming an Optimal Control Problem (OCP) in a Non-linear programming Problem (NLP). State and control variables are approximated in terms of Nth-degree Lagrange polynomials over a non-uniform spaced grid i.e, the Chebyshev-Gauss-Lobatto (CGL) nodes. The choice of CGL nodes as collocation points and Lagrange polynomial as trial functions, leads to achieve the best approximation in term of max-norm over any other interpolating functions.

With regard to the control of the A/C, different solutions are available. Some of these are intended to follow pre-established constant target, whereas others adapt the control of the vehicle to the Air Traffic Management (ATM) contingencies, such as obstacles, air traffic high-density areas, unfavorable weather conditions, etc. In this study, an innovative set of GNC techniques for the FMS of a Boeing 747-100 is presented. With regard to 4DT context, the main purpose of these techniques is to overhaul the Lateral Navigation (LNAV), Time Navigation (TNAV) and Vertical Navigation VNAV of the A/C, to respect the time constraint of the 4DT defined for the last waypoint of a cruise mission. As additional tasks, the FMS is also able to avoid a NFZ, to capture and follow an established route, and finally, to ensure, simultaneously, a minimum fuel consumption trajectory. The NFZ, as well as the cases of re-entry to the established route, can lead to delays in the scheduled time of arrival of the aircraft. The prediction and control of these delays is required in order to avoid an inefficient management of the aircraft performance and airspace. The reasons described above drove the development of new solutions presented in this work. Chapter II presents the numerical method and the A/C model adopted for the solution of the OCP. Chapter III details the guidance navigation and control functions implemented as the kernel of the FMS. Finally, Chapter IV expose the results of the simulations performed by using the Multipurpose Aircraft Simulation Laboratory (MASLab).

II.   The Optimal Control Problem

In general terms, the objective of an Optimal Control Problem (OCP) is to determine the control function $u(t) \in \mathbb{R}^m$ and the corresponding state variables $x(t) \in \mathbb{R}^n$ of a given control system, in order to minimize an user-defined cost function J, where $t \in \mathbb{R}$ is the independent time variable, m is the number of controls and n is the number of states.

The purpose of the OCP described in this work is to find the *minimum-fuel* trajectory which leads an A/C to fly a sequence of waypoints, while respecting the Controlled Time of Arrival (CTA), i.e., the time leeway defined by the ATC when the A/C is expected to arrive at the route final waypoint. To this end, the cost function J can be expressed as the mass of fuel needed for the flight mission, and it assumes the Bolza form:

$$J(x(t), u(t), t) = \Psi\big(x(t_0), t_0, x(t_f), t_f\big) + \int_{t_0}^{t_f} L(x(t), u(t), t)dt \qquad (1)$$

$\Psi\big(x(t_0), t_0, x(t_f), t_f\big)$ is the cost function Mayer term and it depends only on the initial and final value of the state vector, whereas $\int_{t_0}^{t_f} L(x(t), u(t), t)dt$ is the Lagrange term which could be evaluated by numerical quadrature[1]. For the purpose of this work, Lagrange term was neglected.

In order to avoid unfeasible or unrealistic trajectories, the 4DT optimization problem is subject to the A/C dynamic constraints, which in general may be expressed by

$$\dot{x}(t) = f(x(t), u(t), t), \qquad t \in [t_o, t_f] \tag{2}$$

State and control variables are subjected to the simple bounds

$$x_l \leq x(t) \leq x_u \tag{3}$$

$$u_l \leq u(t) \leq u_u \tag{4}$$

whereas boundaries conditions are applied by the inequality relation

$$\psi_l \leq \psi\big(x(t_0), x(t_f), t_f - t_0\big) \leq \psi_u \tag{5}$$

The path constraints are introduced in the problem by the inequality:

$$C_l \leq C(x(t), u(t), t) \leq C_u \tag{6}$$

A. Pseudospectral Method and Nonlinear Programming Problem

In this section the method used for the OCP solution is presented. Various methods are proposed in calculus of variations literature and all of these are gathered in two main groups: the indirect methods, and the direct methods. Whereas the former aim to solve the necessary conditions derived from the Pontryagin minimum principle[2], the latter achieve a discretization of time history and an approximation of both state and control variables using an accurate interpolation scheme. In this paper, the OCP is solved through a Chebyshev pseudospectral method developed by Ross and Fahroo[3], and Elnagar and Kazemi[4]. The basic idea behind this direct collocation method is to transform the ordinary differential equations (ODEs) system into an algebraic equations system, by employing jth-degree Lagrange polynomials for the state and control variables. In this manner the state and control variables can be expressed through their values at the Chebyshev-Gauss-Lobatto (CGL) nodes, and the OCP is transformed into a constrained Nonlinear Programming Problem (NLP).The jth-degree Chebyshev polynomial is defined as the unique polynomial satisfying

$$T_j(t) = \cos(j \arccos(t)) \tag{7}$$

In the Chebyshev pseudospectral method the CGL interpolation nodes are given by

$$t_k = \cos\left(\frac{\pi k}{N}\right), \qquad k = 0, \dots, N \tag{8}$$

These nonuniform spaced nodes lies on the interval $[-1, 1]$ and they represent exactly the $N + 1$ points where extrema of $T_N(t)$ occour. Since the domain of the Chebyshev polynomial is the interval $[-1,1]$, a real time history such as $[t_0, t_f]$ needs to be transformed in the interval $[-1,1]$ by the following linear relation:

$$\tau(t) = \left[\frac{(t_f - t_o)t + (t_f + t_0)}{2}\right], \qquad t \in [-1,1], \tau: [-1,1] \rightarrow [t_0, t_f] \tag{9}$$

For sake of readability, the notation t will continue to refer to $\tau(t)$. The approximation of state and control vector is addressed by using a linear combination of Lagrange polynomial of the form

$$x^N(t) = \sum_{j=0}^{N} x_j l_j \tag{10}$$

$$u^N(t) = \sum_{j=0}^{N} u_j l_j \tag{11}$$

where N is an arbitrary real even or odd, and $N+1$ is the number of CGL points; x_j and u_j are the value of the states and control vectors at the jth CGL nodes and finally, $l_j(t)$ are the Nth-order Lagrangian interpolating polynomial. To obtain an approximation of the derivative $\dot{x}(t)$ at the CGL nodes t_k, Eq.(10) can be differentiated resulting in the following expression:

$$\dot{x}^N(t_k) = \sum_{j=0}^{N} x_j \, \dot{l}_j(t_k) = \sum_{j=0}^{N} D_{kj} x_j, \qquad k = 0, \dots, N \tag{12}$$

where D_{kj} are the entries of a $(N+1) \times (N+1)$ differentiation matrix defined in Ref.(5). The matrix D depends only on the number of CGL nodes, thus once N is fixed D is a constant matrix. The cost function and state equations are discretized by first substituting Eqs.(10), (11), and (12), in Eqs.(1) and (2), and collocating at the nodes t_k. As a result, the OCP problem is traduced in a NLP: a problem aimed to find the arrays of states $X = (x_0, \dots, x_N)$ and controls $U = (u_0, \dots, u_N)$ which minimize the cost function

$$J(X, U, t_f) \approx \Psi(x_0, t_0, x_N, t_N) + \frac{t_f - t_0}{2} \sum_{k=0}^{N} L(x_k, u_k, t_k) w_k \tag{13}$$

subject to

$$\frac{2}{t_f - t_0} \sum_{j=0}^{N} D_{kj} \, x_j = f(x_k, u_k, t_k), \qquad k = 0, \dots, N \tag{14}$$

$$\psi_l \leq \psi(x_0, x_N, t_f - t_0) \leq \psi_u \tag{15}$$

$$C_l \leq C(x_k, u_k, t_k) \leq C_u, \qquad k = 0, \dots, N \tag{16}$$

B. The Aircraft Model

The choice of which particular model is more appropriate to represent A/C dynamics in the optimization problem, is a pretty rocky issue to address. In current literature, in effect, while several examples of A/C dynamics models are given, lacking attention is given on the reason why one model is preferable than others. Essentially, the A/C model is represented by a system of mathematical equations which constraint the A/C state and control variables. In this work the A/C is modeled by a 3 Degree Of Freedom (3DOF) Aircraft Dynamic Model (ADM), which considers both kinematic and dynamic equations. The ADM provides more realistic simulation and accurate description of A/C behavior. Since the computational effort required by the ADM is significant, it can be substituted by a linear simplified model based on steady state flight conditions. The linear model reproduces performance and limitations of the A/C in a steady state condition by using different sets of A/C performance database. The performance steady state data can be extracted from performance calculation tools, such as BADA[6], and the Multipurpose Aircraft Simulation Laboratory (MASLab)[7]. In this study, the steady state performance database is extracted from BADA, and MASLab is only used as flight simulator. The state variables for each CGL node were gathered in a 7-dimension array as

$$x = [N \quad E \quad H \quad m \quad V_{TAS} \quad \gamma \quad \psi] \tag{17}$$

where $N, \ E, \ -H$, are the A/C North-East-Down reference frame coordinates, while m is the gross mass of vehicle, V_{TAS} is the A/C true air speed, γ is the flight path angle, and finally ψ is the heading angle. The mathematical model used to describe the A/C dynamic is expressed by

$$\dot{x} = f(x, u, t) = \begin{cases} \dot{N} = V_{TAS} \cos \gamma \cos \psi \\ \dot{E} = V_{TAS} \cos \gamma \sin \psi \\ \dot{H} = V_{TAS} \sin \gamma \\ \dot{m} = -TSFC(V_{TAS})T(H) \\ \dot{V}_{TAS} = \dfrac{1}{m}(T - D - mg \sin \gamma) \\ \dot{\gamma} = \dfrac{1}{mV_{TAS}}(L \cos \phi - mg \cos \gamma) \\ \dot{\psi} = \dfrac{L \sin \phi}{mV_{TAS} \cos \gamma} \end{cases} \tag{18}$$

where the first three equations represent only the kinematic constraints, $\dot{m}$ is the BADA fuel flow prediction for the cruise phase, ϕ is the roll angle, and the last three equations are the dynamic constraints more representative for the flight mission considered in this study.

C. The Path Constraints

Cruise endpoints, traffic separation aspects, terrain obstacles, weather hazards, noise sensitive areas, and persistent contrail formation region, are all examples of path constraints that can be included in the trajectory optimization problem. In addition to this, the flight plan constraints can be added to the 4DT optimization problem as speed, altitude or time constraints. With the exception of the cruise endpoints and flight plan constraints, the previous path constraints were represented by a No-Fly Zone (NFZ), namely an airspace region or volume with definite boundaries where the flight is restricted or permanently forbidden.

III.   Guidance Navigation and Control Techniques for 4DT

In this section, the set of Guidance Navigation and Control (GNC) techniques for the novel FMS are presented. The main scope of these techniques is to achieve all the functions required for the 4DT navigation:

1) Navigation function, including measurement of A/C states and prediction of the optimized trajectory;
2) FMS and Automatic Flight Control System (AFCS) target generation;
3) Guidance and control functions for the Vertical Navigation (VNAV), Lateral Navigation (LNAV), and Time Navigation (TNAV).

The navigation function is common to all control axes (vertical, lateral and longitudinal axes). The target generation function, instead, needs to focus on which type of control is used for each AFCS axis. In general, the AFCS targets are: the bank angle ϕ_d, the pitch angle θ_d, the Throttle Lever Angle (TLA) Π , the Indicate Air Speed (IAS) target V_{IAS}, and finally, the altitude target H_d. These are the targets provided by GNC algorithms to the AFCS to address the VNAV, the LNAV and the TNAV of a generic 4DT. The schematic of the FMS functions and AFCS-A/C interface are depicted in Figure 1.

A. The Navigation Function and FMS Targets

The assumption to use the states generated by the A/C simulator as measured states strongly simplifies the navigation function. In this approach, the navigation function was essentially reduced in: a mere junction for the A/C states, a navigation database containing the optimized trajectory, and finally in an algorithm to compute the distance flown along the established route i.e., an Along Path Distance (APD) calculator. As far as the last point is concerned, the addition of the time variable to the classical 3D route leads to know, at each time, the APD flown by the A/C along the established route. Indeed, since the OCP solution is a set of time-based A/C states, the FMS has to be able to compute the discrepancy between *where* the A/C is expected to be at the current time, and *where* the A/C effectively is at the current time. In other words, in order to generate targets that are based on the position of the A/C with respect to the established route, the *time-based* OCP trajectory (e.g., $N(t), E(t), H(t), V_{TAS}(t)$, etc.) has to be transformed in a *position-based* trajectory (e.g., $N(R(t)), E(R(t)), H(R(t)), V_{TAS}(R(t))$). The task of calculating the APD $R(t)$ is addressed by a specific algorithm called "APD calculator", whereas the function of expressing the optimum targets $X_{opt}(R(t))$ as a function of the APD flown, is achieved by a series of look-up tables in the FMS targets generation function.

B. The AFCS Targets

In general, an AFCS is meant to provide the air vehicle control surfaces actuators with the necessary commands to fly the A/C toward a specified attitude target. This objective is addressed by activating different control logics, called also "modes", which operate on three distinct A/C control axes: vertical axis (pitch modes), lateral axis (roll modes), and longitudinal axis (autothrottle modes). Table 1 gathers all the MASLab[8] AFCS modes available for each axis of control. At any time, only one single mode can be active for each axis.

The terms "manual" and "managed" depend on whether AFCS is controlled by the pilot or by FMS respectively. For the purpose of this study, only the managed modes were used. In particular, for the pitch axis, VNAV PATH, VNAV SPD or VNAV ALT aims to maintain a desired pitch angle θ_d, an IAS V_{IAS}, or an altitude target H_d respectively.

Type of mode	Pitch	Roll	Autothrottle
Manual	MAN	MAN	THR HOLD
	ALT	HDG	THR REF
	VS	TRK	SPD
	IAS	LOC	MACH
	GS	TOGA	
	TOGA		
Managed	VNAV PATH	LNAV	Managed THR REF
	VNAV SPD		Managed SPD
	VNAV ALT		Managed MACH

Table 1.   Manual and managed modes of the MASLab Automatic Flight Control System.

For the lateral axis, only one managed mode exists and it is aimed to maintain a desired roll angle ϕ_d. Finally, three managed modes are available for the longitudinal axis: THR REF, SPD, and MACH .They can be used to maintain a desired TLA Π_d, an IAS V_{IAS}, or a Mach target M respectively. Since the implementation of the GNC techniques required in 4DT guidance has to work along the same lines of the design of AFCS modes, it was of paramount importance to understand the MASLab AFCS functionalities. For more details concerning how the MASLab AFCS modes work, refer to Ref. (8).

C. The Vertical Navigation

The purpose of the Vertical Navigation (VNAV) is to control the A/C attitude along the vertical axis. Therefore, VNAV has to generate the AFCS targets required to follow a specified vertical profile expressed in terms of altitude target H_d. The AFCS has two targets that can be used for this
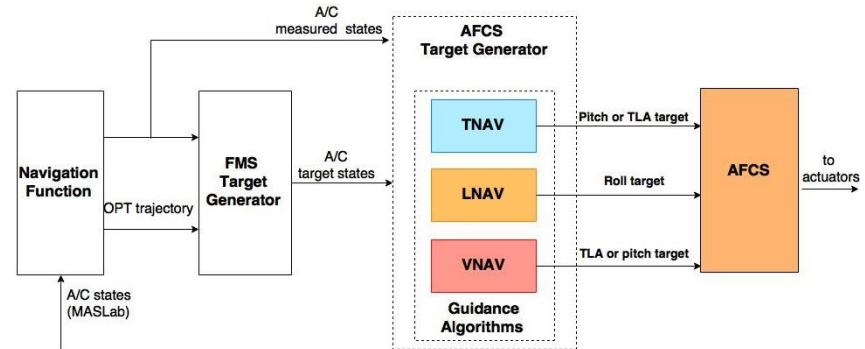

Figure 1. Schematic of the Flight Management System and its context.

purpose: the pitch angle θ and throttle Π. The algorithm used to generate this commands are two, and both use a Proportional-Derivative (PD) controller to contain the altitude error between the OCP target altitude H_d, and the current altitude H of the A/C. When the elevator is chosen to control the altitude, the PD controller generates the pitch angle target θ_d as:
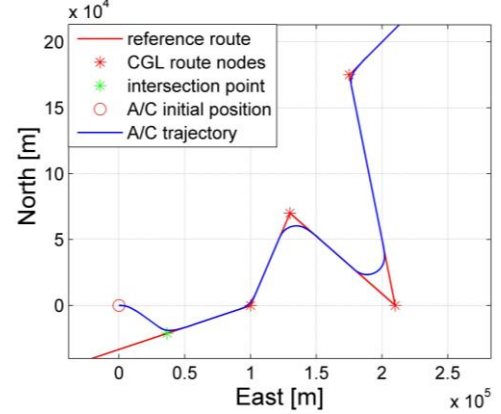

Figure 2. Example of a generic flight mission conducted by the LGM guidance.

$$\Delta H = H_d\big(R(t)\big) - H \tag{19}$$

$$\Delta \theta = \theta_d - \theta = K_p \Delta H + K_d \frac{dH}{dt} \tag{20}$$

where ΔH indicates the altitude error (the difference between the desired altitude H_d and the A/C current altitude H), and K_p and K_d are, respectively, the proportional and derivative gains of the PD controller. The pitch target θ_d is then sent to the VNAV PATH mode of the MASLab AFCS, which is the responsible to send to the actuators the commands needed to follow the desired altitude target.

When the throttle is used to control the altitude of the A/C, the PD controller generates the target Π_d as a function of altitude error similarly to Eq.(20), and Π_d is then sent to the Managed THR REF mode of the AFCS.

D. The Lateral Navigation

The projection of the optimum trajectory of the A/C on the North-East plane, is a sequence of route legs leading from the first waypoint to the last waypoint of the cruise flight plan. In order to track an established route on the lateral-directional plane of the A/C, the FMS should be able to break the directional path into a sequence of basic lateral maneuvers. The Lateral Guidance Manager (LGM) is the main algorithm that addresses this task, and it can be considered as the kernel of the lateral control along the established route. The LGM developed in this work is based on the work did by Peters and Konyak[9].

Once the A/C initial position is well established by Navaids, and route data uploaded in the FMS by the optimization process, the LGM knows all the maneuvers that form the flight plan and it generates the required targets for the LNAV. *Route Following* and *Route Capture* are the principal sets of maneuvers used to control the A/C along lateral axis. By using a combination of these, the A/C can starts from any initial condition and fly until the end of the route. Figure 2 illustrates a generic flight mission conducted by the LGM guidance.

For the sake of conciseness, only the control law used during the Route Following is explained here. During this maneuver, the A/C has to maintain the desired segment course (heading angle) and eliminate the lateral separation from the established route. The lateral separation, here indicated as Cross Track Error (CTE), is processed by a Proportional-Integrative-Derivative (PID) controller, which provides a desired target for the bank angle. The commands provided by the PID, summed to the signals originated by the HDG mode of the AFCS,

produce a desired bank angle based on the magnetic course and on the lateral separation from the route. The control law is mathematically described by the following equation:

$$\Delta\phi = \phi_d - \phi = K_P\Delta\psi + K_{pCTE}CTE + K_{dCTE}\frac{dCTE}{dt} + K_{iCTE}\int CTE\ dt \tag{21}$$

where $\Delta\psi$ indicates the error between the desired heading angle ψ_d and the current A/C's heading angle ψ, K_p is a proportional gain that needs to be scheduled with A/C TAS, whereas $K_{pCTE}, K_{dCTE}, K_{iCTE}$ are, respectively, the proportional, derivative and integrative gains of the PDI controller.

Triggering the target generation for the other control axes is an important aspect of the LNAV. Indeed, in order to generate targets that are position-based, the LNAV should provide the other axis with the information about the relative location of the A/C with respect to the established route. The Route Following guidance for the LNAV represents the best instrument to communicate to other axis which route segment the A/C is currently flying. Figure 3 shows the flow chart implemented in the state machine for the Route Following guidance. The control logic governs the activation of the track-to-fix maneuver and the fly-by maneuver iteratively. When the transition maneuver ends (i.e. when A/C it is aligned with the next route segment), the state machine generates the "shift" signals that advises the passage from the current route leg to the subsequent one.

E. The Time Navigation

In order to completely define a 4DT, each waypoint forming the route must be associated with an Established Time of Arrival (ETA). In this research, the ETA are the CGL time nodes of the OCP solution. The Controlled Time of Arrival (CTA), instead, is the time constraint defined for the initial and last waypoint of the cruise phase. When a CTA is set for the last waypoint of the established path (CTA of the first waypoint is set to simulation time zero), the goal of TNAV is to provide the A/C speed changes needed to contain errors between the CTA and the effective Time Of Arrival (TOA) at the last waypoint. Therefore, the FMS has to generate an airspeed target profile for the AFCS, as well as the control signals required for the longitudinal axis (i.e., pitch angle or the TLA), to respect the time constraints at each waypoint.

The TNAV control law used in this study is a slight modification of the Interval Management (IM) algorithm developed by Bai, Vaddi, and Mulfinger[10]. As a general concept, the IM strategy is aimed to maintain a longitudinal separation between two vehicles (Target A/C and Ownship A/C) during the approach, when they are equipped with ADS-B (Automatic Dependent Surveillance-Broadcast) system. Since no Target vehicle was considered in this work, the longitudinal separation was to set to be equal to the CTA of the last waypoint. As a result of these assumptions, the error in TOA of the Ownship A/C simply is:

$$e_{TOA} = t - t_{opt}(R(t)) \tag{22}$$

where t is the current simulation time and $t_{opt}(R(t))$ is the expected time of arrival based on the reference trajectory (ETA). The time error sign is positive when A/C is delayed and negative when the A/C is anticipating the established route. The speed variation used to reduce the TOA error follows a proportional law of the form
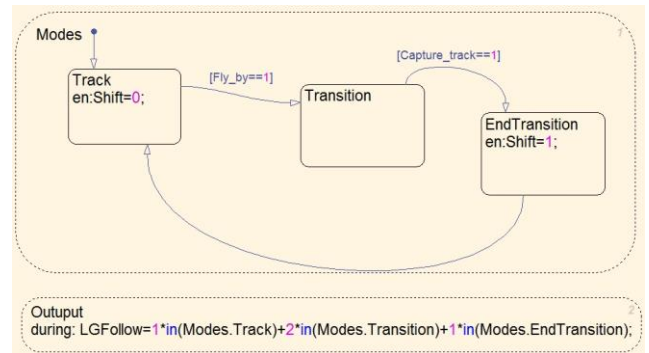

Figure 3. Flow chart of the Route Following guidance.

$$\Delta V = k_v e_{TOA} \tag{23}$$

where the gain k_v has the dimension of an acceleration, and it dictates how much speed variation is commanded per each second of error. The A/C TAS target V_{com} is defined as

$$V_{com} = V_{TAS} + \Delta V, \qquad \Delta V \in [0, 0.1 V_{TAS}] \tag{24}$$

Moreover, in order to prevent strong variations in airspeed target value, the incremental speed command ΔV was bounded to be less than 10% of current A/C TAS.

The IM algorithm used to generate the TNAV targets is therefore represented by the Eqs. (23) and (24). However, the speed target admitted by AFCS is expressed as IAS, so a previous conversion from TAS to IAS is needed. The algorithm described until here is the target generator for the TNAV axis. The control laws used to capture and maintain the speed target values were chosen among the AFCS modes of MASLab. Two control targets can be chosen: the pitch angle θ or the TLA Π. Hence, when the control along longitudinal axis is carry out by the elevator command, the VNAV SPD mode is used; conversely, when speed control is addressed by using the throttle command, the A/T SPD mode is used.

Another interesting task addressed by the TNAV is related to the presence of the NFZ. The optimal cruise trajectory is a discrete sequence of A/C states calculated at the CGL time grid. Thus, the derived reference trajectory is approximated by a piecewise linear curve, which links the CGL nodes in the North-East plane of the A/C. Although the discrete solutions singularly falls outside the NFZ, the flight path between two nodes may cross the NFZ. In order to avoid the NFZ during the flight, an additional waypoint is needed. The additional waypoint is positioned at the intersection of two segments tangent to the NFZ. This situation is represented in Figure 4. Since the additional waypoint is not part of the OCP solution, the optimal states in that point have to be extrapolated. Whereas the mass and altitude values were interpolated linearly, the generation of the TAS target is governed by the *spread* algorithm. The strategy is to produce different TAS profiles, depending on the number of waypoints after which the A/C want to recover the delays due to the NFZ detour. If n_{split} is the number of waypoints (after the additional one) after which the A/C would have to respect the optimum time constraint $t_{opt}(R(t))$, $\bar{V}_{TAS}$ is the constant speed that has to be maintained to recover the delay due to the detour. $\bar{V}_{TAS}$ target for n_{split} nodes is obtained by using the simple cinematic relation
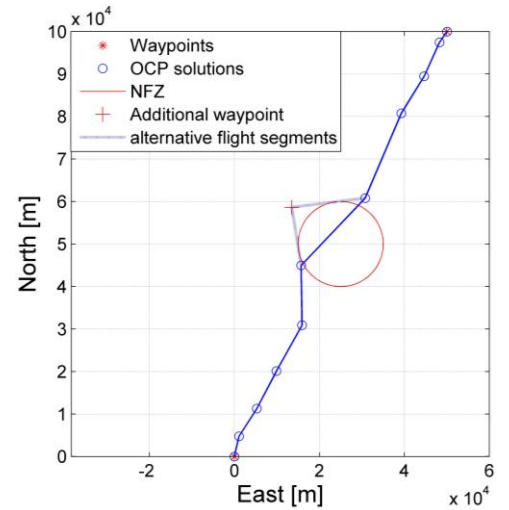

Figure 4. Example of optimum trajectory crossing the NFZ.

$$\bar{V}_{TAS} = \sum_{k=1}^{n_{split}+1} ldev_k/(t_{n+n_{split}} - t_n) \tag{25}$$

where $ldev_k$ is the length of the kth-leg considered in NFZ detouring, and t_n is the CGL node in which deviation should start.

IV. Results

The results of the optimal cruise simulation are presented in this section. The mission was to guide an A/C from the initial waypoint WP_i until the terminal waypoint WP_f of the cruise phase, satisfying the time constraint, minimizing the fuel consumption, and avoiding a NFZ placed along the cruise path. The Above Ground level (AGL) of the cruise endpoints was set to 10887 m. The NFZ was envisaged as a cylinder of radius 10 km with no lower and upper bounds and centered in the point of coordinates [100km North, 100Km East], so that its projection on the North-East plane is a 2D circular area. The CTA at WP_f was set to 2000 s, and it was calculated as the time needed to fly from the first waypoint to the last waypoint of in straight line, maintaining a cruise TAS of 242 m/s. The different GNC algorithms were combined in order to accurately observe the A/C behavior when TNAV, LNAV, and VNAV are operating simultaneously. For each axis of control, a target generator and an AFCS mode (as interpreter of the targets) have to be chosen. Depending on which mode is used for each axis, three FMSs were developed:

1. **FMS #1**
   VNAV - AFCS mode: VNAV ALT (θ_d); target generator: none, the target is directly H_d;
   LNAV - AFCS mode: LNAV (ϕ_d); target generator: Lateral Guidance Manager (LGM);
   TNAV - AFCS mode: A/T SPD (Π_d); target generator: Interval Management (IM);
2. **FMS #2**
   VNAV - AFCS mode: VNAV PATH (θ_d); target generator: PD controller;
   LNAV - AFCS mode: LNAV (ϕ_d); target generator: LGM;
   TNAV - AFCS mode: A/T SPD (Π_d); target generator: IM;
3. **FMS #3**
   VNAV - AFCS mode: A/T Managed THR REF (Π_d); target generator: PD controller;
   LNAV - AFCS mode: LNAV (ϕ_d); target generator: LGM;
   TNAV - AFCS mode: VNAV SPD (θ_d); target generator: IM.

The FMS#2 differs from the FMS#1 only on the VNAV target generator. Since no relevant differences were observed between them, the simulation results related to the FMS#2 are omitted. The FMS#1 and FMS#3 differs only on the command used to control the attitude and the speed of the A/C. Whereas the FMS#1 adopt the strategy "speed-on-throttle" and "path-on-elevator", vice versa for the FMS#3, that uses the throttle to control the altitude and elevator to control the speed. Table 2 contains the data which define the optimum reference 4DT. The symbol "+" refers to the additional waypoint and ETA are calculated for n_{split} equal to one. Figure 5 represents the projection of the A/C trajectory on the North-East plane when FMS#1 is adopted in the simulation.

Since the three FMSs implement the same algorithm for the LNAV, the A/C trajectory on the North-East plane is

CGL	1	2	3	4	+	5	6	7	8	9	10	11
North [km]	0	8.4	33	72.16	111	122.52	180	238.13	286.56	321.93	344.65	353
East [km]	0	8.4	33	72.16	90	122.49	180	238.13	286.58	321.94	344.66	353
AGL[km]	10.89	10.89	10.89	10.89	10.92	10.95	10.89	11.27	11.73	11.61	11.22	10.89
ETA [s]	0	49	191	412	566	691	1000	1309	1588	1809	1951	2000

Table 2.   Optimum reference trajectory at the CGL.

CGL	1	2	3	4	+	5	6	7	8	9	10	11
ETA [s]	0	49	191	412	566	691	1000	1309	1588	1809	1951	2000
TOA [s]	0	49	191	412	574	699	1003	1312	1588	1807	1950	2000
e_{TOA} [s]	0	0.2	0.2	0.3	7.2	8	3.2	2	0	-2.3	-1.1	0.2

Table 3.   Time results adopting the FMS#1.

the same regardless of which FMS is used. Table 3 collects the relative errors in TOA. If RNAV 2 is imposed longitudinally[11,12] on the last waypoint, the A/C exceeds the longitudinal limit only during 10.05 s. When comparing this interval with the total duration of the simulation (2000 s), the flight is in compliance with the RNAV requirements. FiguresFigure **6** and Figure **7** show the target profiles followed by the FMS#1 for two cases. The trend of V_{TAS} target depends on how many waypoint are chosen to spread the NFZ avoidance in space and in time. When n_{split} is one (Figure 6), the LNAV accelerates the A/C to recover the reference TOA on the first waypoint after the NFZ. The sharp peak in correspondence of the additional waypoint could lead the A/C beyond the envelope limits. To solve this problem, and create a smoother speed profile, n_{split} was set to be equal to three (Figure 7).

When comparing Figures Figure **7** and Figure **8**, the speed profile followed by FMS#3 is more accurate. This is the results of using the elevator command to control the speed. Indeed this control has a faster response in targeting the speed profile than the "Speed-on-Throttle" strategy of FMS#1. Figure 9 shows the trend of the A/C gross weight during the simulation with the FMS#1. There is a strong divergence between the A/C's gross mass established by MASLab simulator (blue line), and the mass value established by the OCP (red dotted line). The total fuel consumption predicted by the OCP was 6284.8 kg, whereas the fuel burned estimated by MASLab during the cruise mission was 7442 kg. The error (1157.1 kg) represents almost 16% of the total fuel burned. The cause of this error stems from two reasons: the presence of a NFZ, and the discrepancies between the OCP fuel consumption model (BADA) and the model embedded in MASLab. As far as the first reason is concerned, the deviation due to the NFZ, as well as the speed changes aimed to respect the time constraint over the NFZ, are all aspects not considered by the optimization process. Further, both BADA and MASLab models are not perfect, so they cannot perfectly predict the fuel consumption at each instant of cruise mission.

Finally, to observe the effectiveness of the LGM when the A/C has to be guided from any initial location to the WP_f, an additional scenario was analyzed. In this scenario, the A/C location is far from the initial waypoint, and the A/C heading angle is a random value. Figure 10 shows the A/C 2D trajectory when FMS#3 is chosen for this scenario, and Table 4 contains the time results. Considering the ability of the IM algorithm to decelerate and accelerate properly the A/C, the CTA on WP_f was respected also in this case.
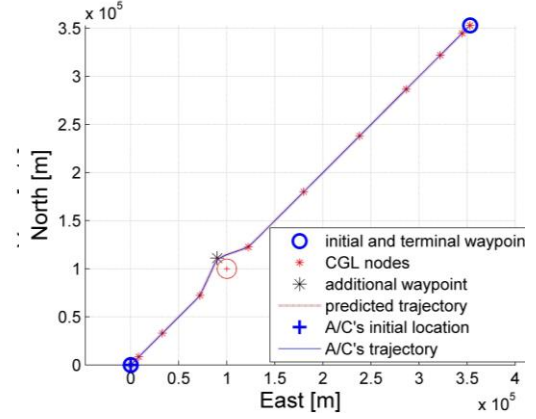

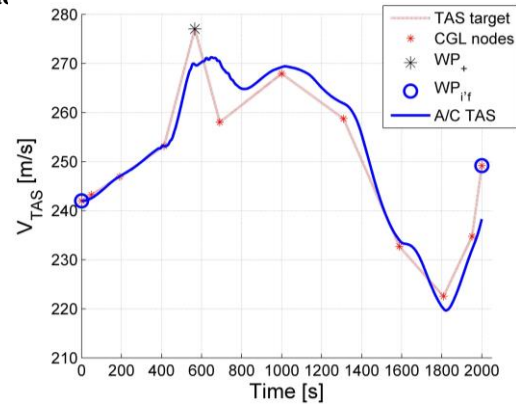Figure 5. Projection of the A/C trajectory on the North-East plane.

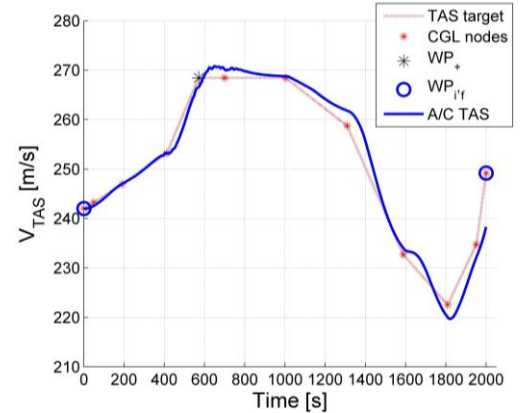Figure 6. TAS target and A/C TAS profile adopting the FMS#1 and $n_{split} = 1$.

Figure 7. TAS target and A/C TAS profile adopting the FMS#1 and $n_{split} = 3$.

V. Conclusion

The results of MASLab simulations showed, in the first place, a satisfactory aptitude of the innovative LNAV and TNAV control techniques to perform a 4DT navigation. In particular, the results showed that LNAV is the best solution to communicate to the other control axis the transition between the different route legs. Secondly, the results demonstrated a strong adherence with time windows defined for the 4DT along the longitudinal axis, especially when FMS#3 is adopted. The work done is not exhaustive for the flight simulation context, as well as for

CGL	1	2	3	4	+	5	6	7	8	9	10	11
ETA [s]	0	49	191	412	571	700	1003	1309	1588	1809	1951	2000
TOA [s]	n/a	n/a	n/a	369	545	678	991	1308	1588	1809	1950	1999
e_{TOA} [s]	n/a	n/a	n/a	-43	-26	-22	-12	-1	0.6	-0.5	-1	-1

Table 4. **Time results adopting the FMS#3 for the second scenario.** *The ETA are calculated for n_{split}=3.*

the field of trajectory optimization. The LNAV could be enhanced by defining new lateral maneuvers e.g., fly-over waypoints and holding patterns. Further works are needed to address route optimization processes able to consider dynamic 3D NFZ, multi A/C scenarios, as well as real atmosphere and wind model scenarios. Finally, the control techniques for optimum targeting developed in this work need to be improved, and/or extended.

References

[1]Clenshaw, C. W., and Curtis, A. R., "A Method for Numerical Integration on an Automatic Computer", *Numerische Mathematik,* Vol. 2, 1960, pp.197-205.

[2]Pontryagin, L. S., Boltyanskii, V. G., Gamkrelidze, R. V., and Mishchenko. E. F., "The Mathematical Theory of Optimal Processes", Wiley-Interscience, 1962.

[3]Fahroo, F., and Ross, M., "Direct Trajectory Optimizaton by a Chebyshev Pesudospectral Method", *Journal of Guidance, Control and Dynamics*, Vol.5, No.1, 2002.

[4]Elnagar, G. N., and Kazemi, M. A., "Pseudospectral Chebyshev Optimal Control of Constrained Nonlinear Dynamical Systems", *Computational Optimization and Applications*, pp.195-217, 1998.

[5]Lloyd, N. T., *Spectral Methods in Matlab*, Society for Industrial and Applied Mathematics, Philadelphia , PA, 2000, pp.1-8

[6]EUROCONTROL, "User Manual For The Base Of Aircraft Data (BADA)", Revision 3.10, 2012

[7]Cassaro, M.,Gunetti, P., Battipede, M., Gili, P., "Overview of the Multipurpose Aircraft Simulation Laboratory Experience", AIAA 2013 Aviation Technology, Integration, and Operations Conference, Las Angeles, CA, USA,2013

[8]Gunetti, P., Cassaro, M., Battipede, M., and Gili, P., "Modeling Autopilot Suites For A Multi-Aircraft Simulator", *AIAA Modeling & Simulation Technology Conference,* AIAA, Washington, DC, 19 August 2013

[9]Peters, M., Konyak, M. A., "The Engineering Analysis and Design of the Aircraft Dynamics Model For the FAA Target Generation Facility", Simulation Branch, Laboratory Services Division, Federal Aviation Administration, Oct. 2012.

[10]Bai X., Vaddi S., Mulfinger D., "Evaluation of Temporal Spacing Errors Associated with Interval Management Algorithms", *14th AIAA Aviation Technology, Integration, and Operations Conference*, AIAA, Washington, DC ,16-20 June 2014

[11]ICAO, "ICAO Doc. 8168, Aircraft Operations, Volume II, Construction of Visual and Instrument Flight Procedures", Fifth edition, Montréal, 2006

[12]ICAO, "ICAO Doc. 9613, Performance-Based Navigation (PBN) Manual", Fourth Edition, Montréal, 2013.
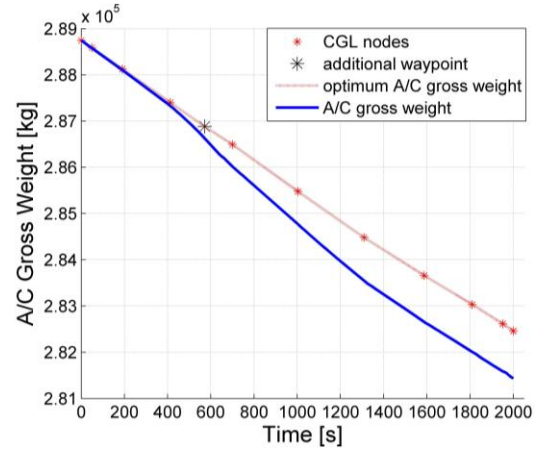
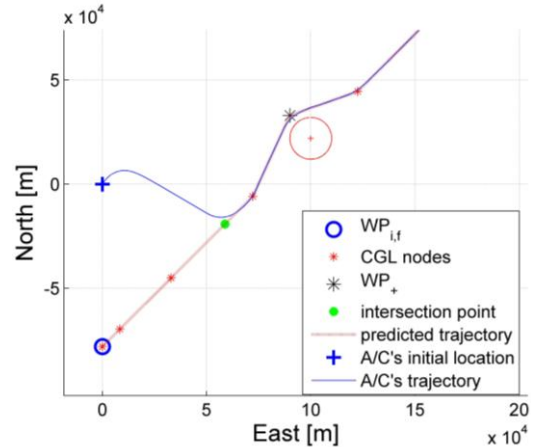**Figure 9. A/C gross mass adopting the FMS#3 and $n_{split} = 3$.**

Figure 10. Projection of the A/C trajectory on the North-East plane for the second scenario.

12